Int J Clin Exp Pathol 2017;10(5):5379-5392
www.ijcep.com /ISSN:1936-2625/IJCEP0039983

Original Article

Modulation of the lung RNAome in a metabolic syndrome rat model

Sofia M Rodríguez-Peredo[1,2], Ashley K Castellanos-Jankiewicz[1], Ivan Imaz-Rosshandler[1], Miguel A Espinoza-Camacho[1,7], Claudia Rangel-Escareño[4], José L Muñoz-Sánchez[2], Jorge Melendez-Zajgla[5], M Elizabeth Tejero[1], Roxana Carbó[3], Vilma Maldonado[6], Laura del Bosque-Plata[1]

[1]Laboratorio de Nutrigenética y Nutrigenómica, Instituto Nacional de Medicina Genómica, Periférico Sur No. 4809, Col. Arenal Tepepan, Tlalpan, C.P. 14610, Ciudad de México, México; [2]Escuela Nacional de Ciencias Biológicas, Instituto Politécnico Nacional, Prolongación de Carpio y Plan de Ayala S/N, Col. Santo Tomás, Miguel Hidalgo, C.P. 11340, Ciudad de México, México; [3]Departamento de Biomedicina Cardiovascular, Instituto Nacional de Cardiología "Ignacio Chávez", Juan Badiano #1, Col. Sección XVI, Tlalpan, C.P. 14080, Ciudad de México, México; [4]Laboratorio de Genómica Computacional, Instituto Nacional de Medicina Genómica, Periférico Sur No. 4809, Col. Arenal Tepepan, Tlalpan, C.P. 14610, Ciudad de México, México; [5]Laboratorio de Genómica Funcional, Instituto Nacional de Medicina Genómica. Periférico Sur No. 4809, Col. Arenal Tepepan, Tlalpan, C.P. 14610, Ciudad de México, México; [6]Laboratorio de Epigenética, Instituto Nacional de Medicina Genómica. Periférico Sur No. 4809, Col. Arenal Tepepan, Tlalpan, C.P. 14610, Ciudad de México, México; [7]Posgrado en Ciencias Biológicas, Universidad Nacional Autónoma de México, Av. Universidad 3000, Coyoacán, C.P. 04510, Ciudad de México, México

Received September 9, 2016; Accepted December 10, 2016; Epub May 1, 2017; Published May 15, 2017

Abstract: Metabolic syndrome (MetS) is characterized by a constellation of conditions that increase the risk for heart disease and other health problems. Although multiple organs are affected by this syndrome, research that focuses on the organs that are not directly involved in metabolism is lacking. Because MetS increases the risk for various lung diseases, we explored the effects of MetS on the lung in this study. We observed that the chronic consumption of a high sucrose diet for 24 weeks induced MetS in a rat model. Concomitant expression changes in 1,026 coding genes and two microRNAs were observed in the analyzed lung tissues. A network analysis showed degradation changes in the melatonin pathway, which plays a protective role in the lung; impairments of several inflammatory pathways (i.e., interferon-γ and nuclear factor kappa B) were also revealed. Moreover, multiple olfactory genes were unexpectedly deregulated. Overall, the lungs of MetS mice exhibited an inflammatory phenotype with molecular changes that affected several signaling pathways that were related to melatonin metabolism, olfactory receptors and cytokine production. Additional research will be necessary to dissect a possible mechanism for the effects of this syndrome on the lung.

Keywords: Metabolic syndrome, lung, rats, RNAome, high sucrose diet

Introduction

Metabolic syndrome (MetS) is a cluster of risk factors that contribute to the development of diabetes mellitus and/or cardiovascular disease. According to the International Diabetes Federation (IDF), this cluster is characterized by central obesity, insulin resistance (IR), dyslipidemia (elevated triglyceride and low density lipoprotein levels and decreased high density lipoprotein levels), and high blood pressure [1]. This syndrome may result from an unbalanced diet that is high in fat and carbohydrates, along with the patient's genetic background [2, 3].

Adipose tissue serves as an energy storage mechanism and exhibits endocrine functions. Adipose tissue cells secrete adipokines that are involved in regulating appetite, satiety, inflammation, and insulin sensitivity. The effects of adipokines on the circulating levels of leptin and adiponectin during obesity are well known. Several adipokines also play important roles in establishing low-grade chronic inflammation; adipocytes and other cells that are present in adipose tissue secrete pro-inflammatory cytokines, which produce various effects throughout the body [2-5].

Table 1. Physiological parameters

	Control n=12	MetS n=12
Weight (g)	536.3 ± 13	482.6 ± 19
Blood pressure (mmHg)	121.1 ± 4.16	129.4 ± 4.0
Glucose (mg/dL)	89.2 ± 6	88.5 ± 7.1
Cholesterol (mg/dL)	68.5 ± 4.6	52.3 ± 5.3**
HDL-Cholesterol (mg/dL)	46.33 ± 3.2	31.1 ± 3.3***
Triglycerides (mg/dL)	87.8 ± 4.9	136.6 ± 15.07**
Insulin (µUl/mL)	3.7 ± 0.9	5.2 ± 0.7
Adiponectin (µg/mL)	14.2 ± 1.2	33.6 ± 3.6***
Leptin (ng/mL)	0.6 ± 0.06	1.4 ± 0.2**
HOMA	0.8 ± 0.2	1.1 ± 0.1

Each value is presented as the mean plus or minus the standard error (S.E.). **P<0.01; ***P<0.001. HDL: high density lipoproteins; HOMA: Homeostasis Model Assessment.

Changes in insulin signaling during MetS have direct effects on vascular endothelial cells; this extends beyond the regulation of blood flow and includes abnormal cellular signaling in the arteries and in other cell types. These changes contribute to the development of heart disease. Similarly, MetS creates an important dysfunction in pancreatic β cells that leads to type 2 diabetes [6, 7]. This syndrome also has various effects on other organs, such as the liver and kidney. Consequently, MetS strongly contributes to the prevalence of non-communicable diseases, such as cardiovascular disease, type 2 diabetes, non-alcoholic liver disease, and cancer [6, 8-10].

Evidence suggests that MetS is a condition that increases the risk for different lung diseases. Diminished lung functions have been reported in several MetS patients who were assessed by spirometry. Additionally, there are associations with insulin resistance (IR), an increase in body mass index (BMI), abdominal obesity and systemic inflammation (i.e., high levels of C reactive protein) [11-13]. Various features of MetS, such as abdominal obesity, hypertension and pro-inflammatory cytokines, have been associated with diseases such as asthma [14-16]. Additionally, several clinical studies have reported that abdominal obesity, hyperglycemia and elevated levels of systemic inflammatory markers, which are components of MetS, are significantly more prevalent in patients with chronic obstructive pulmonary disease [17-20].

Finally, the mechanisms and endocrine alterations that may elicit specific changes to cellular signaling and gene expression, which would potentially contribute to the increased risk of lung diseases in patients with MetS, remain unknown. In this study, we evaluated morphological and transcriptomic changes in the lung tissues of a diet-induced animal model for MetS.

Results and discussion

In this study, a high-sucrose diet induced dyslipidemia (increased triglyceride (TG) levels and decreased high density lipoprotein-cholesterol (HDL-C)) in rats with MetS. Interestingly, this group exhibited increased leptin and adiponectin levels (**Table 1**). However, these rats also exhibited lower body weights relative to the control (CTL) rats, but the amount of retroperitoneal adipose tissue was approximately doubled. This condition occurred because the MetS animals ate 1/3 of the total food (measured in grams) compared with the CTL animals [21]; thus, they were malnourished, and the carbohydrates they did eat were converted to fat. As expected, we observed that the MetS group exhibited blood pressure, insulin level and homeostasis model assessment (HOMA) index increases compared with the CTL group. However, the differences were not statistically significant; this was likely due to the size of each group [21] (**Table 1**).

The high sucrose diet promoted a redistribution of the retroperitoneal adipose tissue with increased deposits of adipose tissue (AT) to areas around the heart and thoracic cavity, the sternum, and between the lung lobes. Several of these animals contained small lesions in their lung tissues (**Figure 1A**).

The dietary composition plays important roles in the onsets of specific diseases, such as diabetes, obesity and MetS [22, 23]. In our model, the appearance of dyslipidemia and the accumulation of AT confirmed that the high sucrose intake induced metabolic changes in the liver and led to an AT redistribution. Thus, this model achieved at least three IDF criteria [1] and consequently fulfilled the proposed criteria that were established by Kennedy et al. in 2010 for a definition of MetS for rodents [24].

Additionally, histological staining revealed that the lungs from the MetS group exhibited

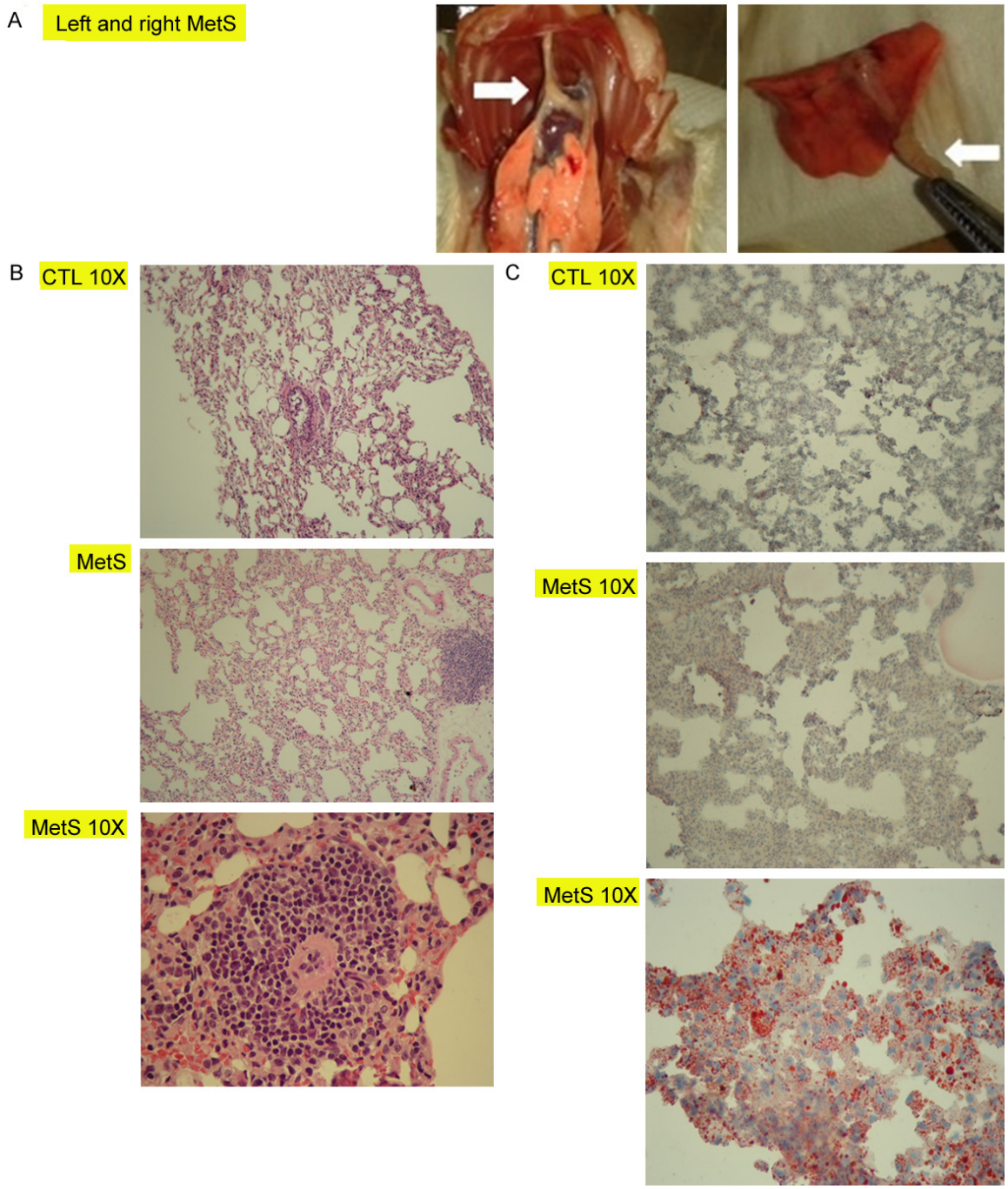

Figure 1. Lung tissue. A. Representative images of lung tissues from the MeTS group. The arrows indicate adipose tissue around the heart (left panel) and lungs (right panel). B. H&E-stained histological lung tissue sections for the CTL and MetS groups. C. RO-stained histological lung tissue sections for the CTL and MetS groups.

increased inflammatory foci with areas of lymphocyte infiltration (**Figure 1B**) relative to the CTL group. Seven rats (7 out of 7) with MetS were positive for RO staining, which confirmed the presence of the lipid content, and most samples were positive for macrophages (**Figure 1C**). One case in the control group was RO positive (1 of 7).

Abnormalities in lipid metabolism have been associated with various pulmonary diseases, including chronic obstructive pulmonary disease (COPD) and lung cancer [25, 26]. AT contributes to systemic pro-inflammatory effects through adipokine secretion. The altered AT deposition (adjacent to the thoracic cage and pericardium) may locally contribute, *per se*, to a deregulation

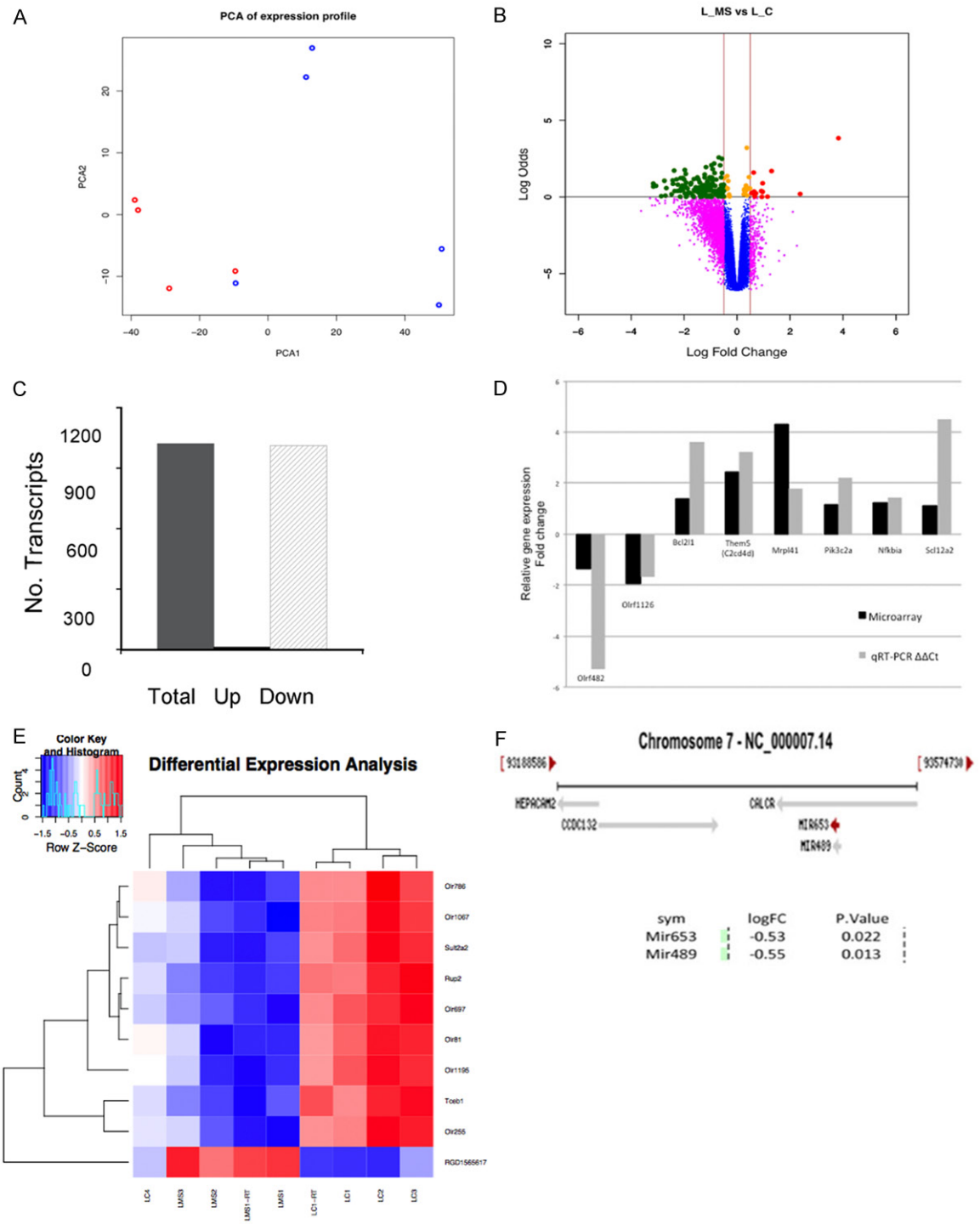

Figure 2. Expression profile. A: PCA plot of total gene expression. The red spots indicate MetS, and the blue spots indicate CTL; B: A volcano plot of the expression differences between the 2 groups; C: Differentially expressed genes; D: Validation of gene expression; E: Deregulated miRNAs in the data matrix; F: Chromosome positions and log FC values of the deregulated miRNAs.

of tissue physiology and molecular pathways by mechanical and paracrine factors. In COPD patients, the tissue secretions of these cytokines correlate with disease severity [27].

Table 2. Top 5 canonical pathways

Name	*p*-value
Melatonin degradation I	4.87E-03
Super pathways of melatonin degradation II	7.35E-03
Thyroid hormone metabolism II	1.56E-02
Nicotine degradation III	1.67E-02
Nicotine degradation II	3.04E-02

Adiponectin and leptin molecules modulate innate and adaptive immune responses [3, 28]. Multiple studies have identified a relationship between the severity of the decrease in lung function that is associated with several conditions, such as asthma and COPD, and high levels of these adipokines [13, 27, 29-32]. Otabe et al. showed that hyperadiponectinemia has anti-inflammatory effects and may slow the acceleration of the aging process that is associated with metabolic syndrome by inhibiting AKT signaling, thereby attenuating the chronic low-grade inflammation that is attributed to the syndrome [33].

To the best of our knowledge, this is the first report to demonstrate that the ingestion of a high sucrose diet promotes important lung tissue alterations. Although it remains unknown, one possible mechanism for these findings may involve the high levels of carbon dioxide that are produced by sucrose metabolism, which would trigger different cell signaling cascades to promote an inflammatory response. In patients with COPD, the international dietary recommendation indicates that the intake of simple carbohydrates should be reduced to improve lung health [34]. Forno E et al. have recently shown that obesity, insulin resistance, and metabolic syndrome may lead to a worsening of lung functions in adolescents with and without asthma. Further research will be needed to understand the underlying causes of these associations [35].

We also analyzed gene expression changes in the lung samples of the rats that were exposed to sucrose. The principal component analysis graph in **Figure 2A** shows two sample groups; each group is differentiated by its global gene expression pattern. After normalization of the raw data using the standard robust-multi-array average (RMA) method, a major subexpression of the total transcript number in the lungs from MetS was identified (volcano plot, **Figure 2B**). In one comparison, 1,026 genes were differentially expressed between the MetS and CTL groups. Thirteen genes were up-regulated, and 1,013 genes were down-regulated, with a *p*-value <0.02 and a log FC>0.58 (**Figure 2C**). To validate the microarray data, we measured the expression of 8 genes by qRT-PCR (**Figure 2D**).

We identified two deregulated miRNAs (mir-653 and mir-489) with a log FC=-0.5. mir-653 is associated with fetal lung development in Sprague-Dawley rats [36], and mir-489 has a potential role in the development of non-small cell lung cancer. Inhibition of the latter promotes cell invasion and regulates the epithelial mesenchymal transition (EMT) in rats [37]. **Figure 2E** shows a heat map of the genes that were deregulated in the two experimental groups, and **Figure 2F** shows the chromosome positions and log FC values of the deregulated miRNAs. The prediction analysis shows 331 transcripts with conserved sites for miR-653-5p and 209 transcripts with conserved sites for mir-489-3p [38]. It will be necessary to conduct further studies regarding the metabolic pathways that are regulated by these miRNAs to better understand the mechanisms that underlie genomic lung transcription.

We performed an enrichment analysis with these data using the IPA software. **Table 2** shows that the melatonin degradation pathway 1 and the melatonin super pathway of degradation 2 were among the top 5 pathways. Melatonin is a widely distributed hormone that plays functional roles in determining sleep patterns and circadian synchronization. Melatonin also exhibits antioxidant activity. In addition to its role as an activator and antioxidant enzyme, it acts as a major, direct scavenger of free radicals [39-42].

The possible involvement of melatonin in the genesis of MetS-mediated lung alterations is indirectly supported by several previous studies. In 2012, Matos et al. found that a melatonin treatment reduced lung oxidative stress and improved dyspnea in a randomized, double-blind, placebo-controlled study of COPD patients [43]. Additionally, Baik et al., demonstrated that melatonin had a protective effect against lung inflammation after measuring pro-inflammatory cytokine levels (i.e., interleukin (IL)-1B, IL-6, tumor necrosis factor (TNF)-alpha, interferon gamma (IFN-γ)) and leukocyte accumulation in the serum and Broncho alveolar lavage fluid (BALF) of mice with lipopolysaccha-

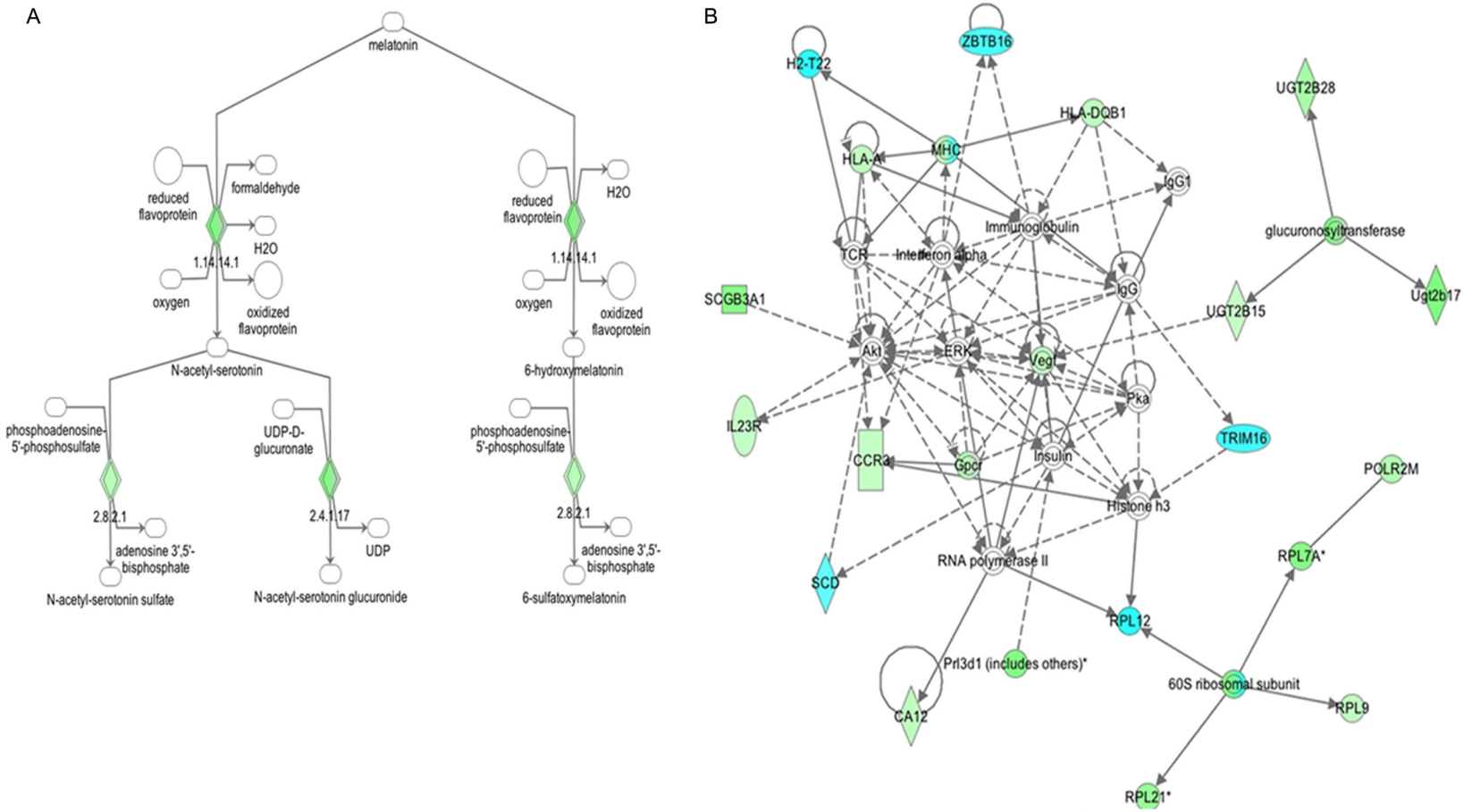
A
melatonin
reduced flavoprotein
formaldehyde
H2O
1.14.14.1
oxygen
oxidized flavoprotein
N-acetyl-serotonin
phosphoadenosine-5'-phosphosulfate
2.8.2.1
adenosine 3',5'-bisphosphate
N-acetyl-serotonin sulfate
UDP-D-glucuronate
2.4.1.17
UDP
N-acetyl-serotonin glucuronide
reduced flavoprotein
H2O
1.14.14.1
oxygen
oxidized flavoprotein
6-hydroxymelatonin
phosphoadenosine-5'-phosphosulfate
2.8.2.1
adenosine 3',5'-bisphosphate
6-sulfatoxymelatonin
B
ZBTB16
H2-T22
HLA-DQB1
HLA-A
MHC
IgG1
Immunoglobulin
TCR
Interferon alpha
IgG
SCGB3A1
Akt
ERK
Vegf
Pka
IL23R
CCRa
Gpcr
Insulin
TRIM16
Histone h3
SCD
RNA polymerase II
RPL12
Prl3d1 (includes others)*
CA12
60S ribosomal subunit
RPL9
RPL21*
UGT2B28
glucuronosyltransferase
UGT2B15
Ugt2b17
POLR2M
RPL7A*

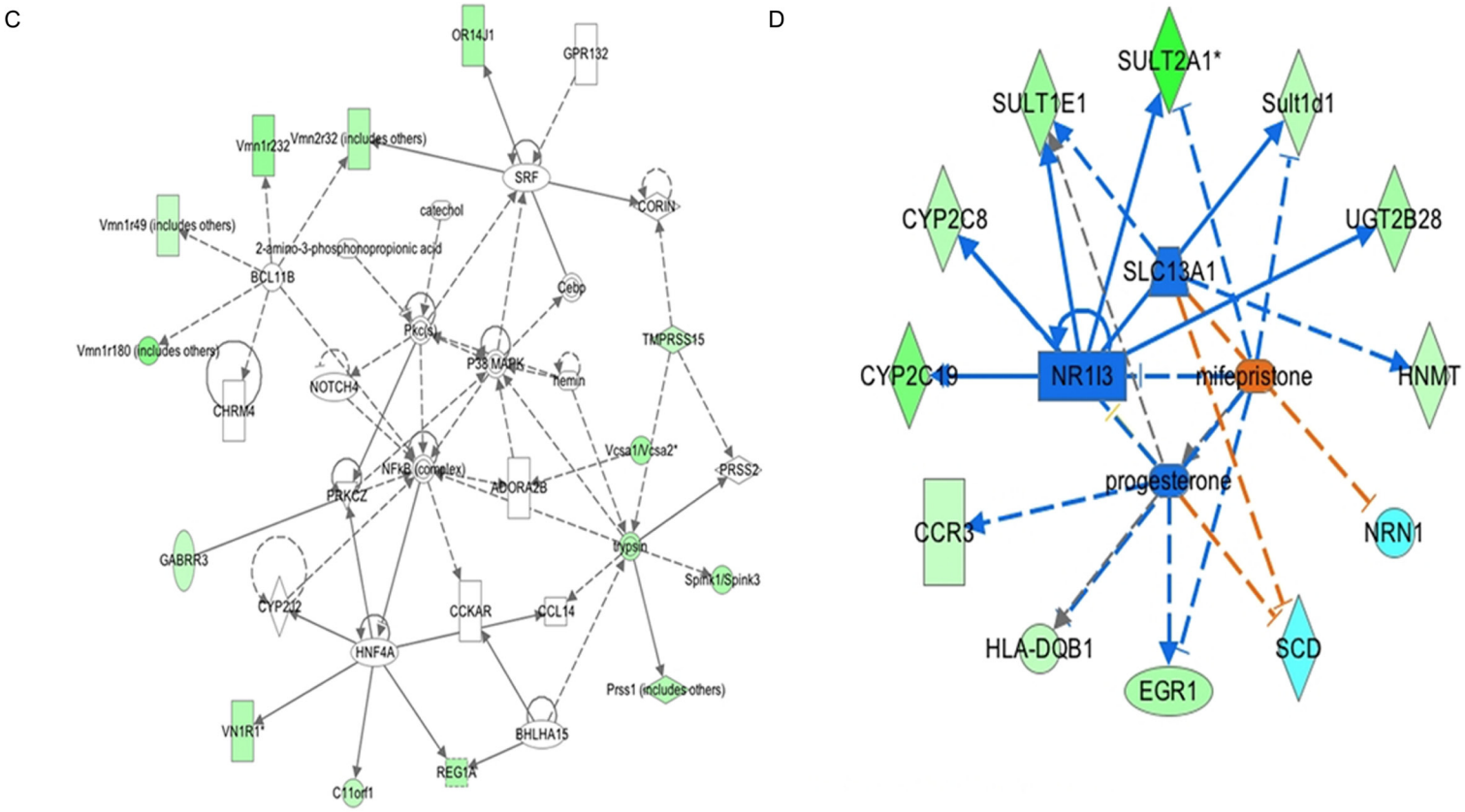

Figure 3. Deregulated transduction pathways in MetS. A: Melatonin degradation pathway; B: Deregulated genes in IFN-γ pathway; C: Deregulated genes in the nuclear factor kappa B pathway; D: Genes that were deregulated by progesterone. Green indicates down-regulation of expression, and blue represents the predicted function of the gene.

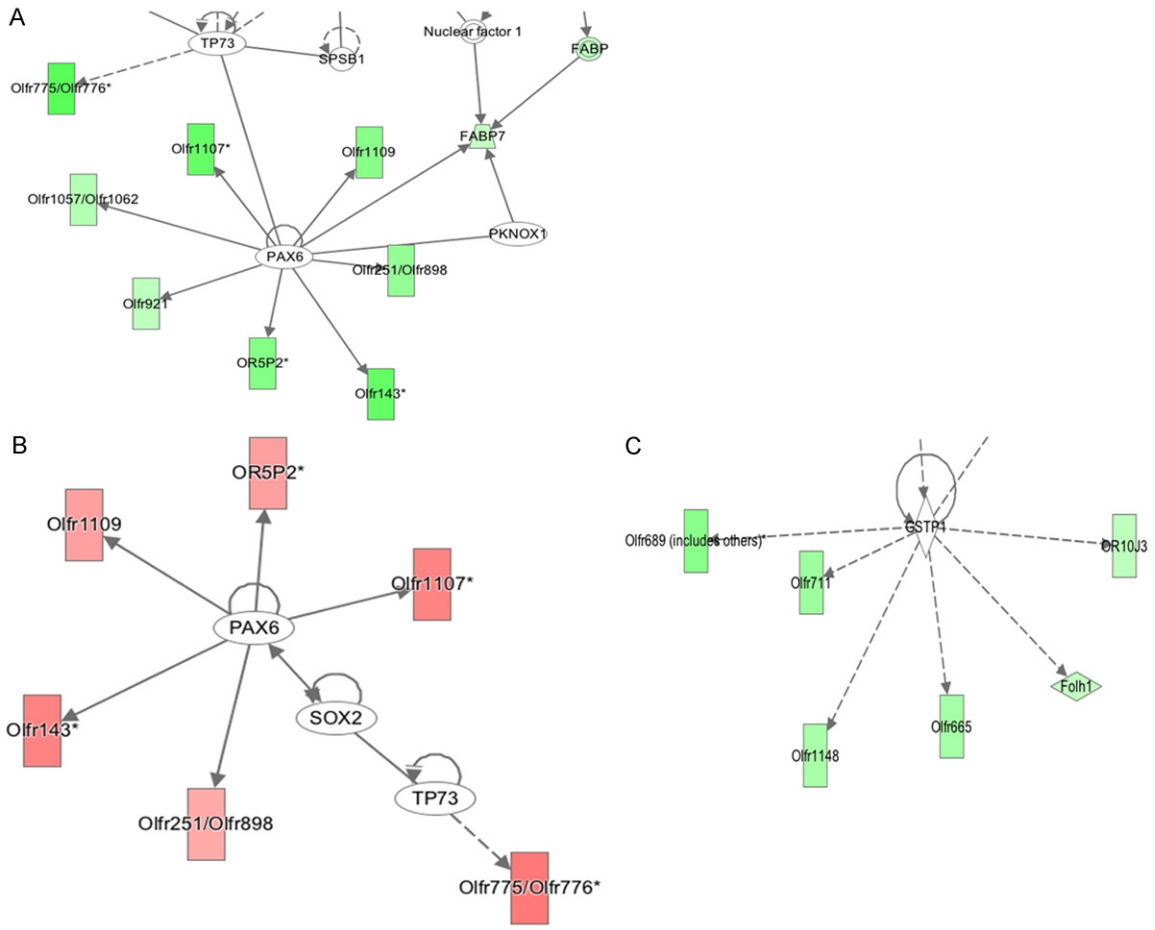

Figure 4. Olfr gene deregulation in rats with MetS. A and B: Olfr regulation network by Pax6; C: Olfr regulation network by Gst.

ride- and sleep deprivation-induced lung inflammation [44]. This may support the notion that a protective pathway is activated as a consequence of the syndrome.

Endogenous melatonin in the lungs reduces oxygen-induced oxidative stress in rats [45]. Generally, melatonin is beneficial to inflammation in lung diseases [43]. However, we hypothesize that the involvement of the deregulated melatonin degradation pathway may affect the lungs through the serotonin pathway because several of the deregulated enzyme transcripts (**Figure 3A**) also affect serotonin production and processing; serotonin is a critical hormone to lung endothelial function [46]. Our results are the first to demonstrate that the deregulation of the melatonin pathway in MetS is potentially associated with pulmonary alterations.

Similarly, we identified several deregulated molecules that were associated with inflammatory pathways, including the histocompatibility complex (MHC), zinc finger and BTB domain containing 16 (ZBTB16), and chemokine (C-C motif) receptor 3 (CCR3); they are linked to the IFN-γ pathway (**Figure 3B**). We also identified several other deregulated genes, including the vomeronasal receptors (vmnrs) (**Figure 3C**). These receptors are indirectly associated with the nuclear factor kappa B (NF-κB) pathway, and this transcription factor may be involved in the inflammatory responses of the lungs in the MetS rats. Notably, several genes that are regulated by progesterone and glucocorticoids were also altered in the MetS rat lungs in the microarray analysis (**Figure 3D**), which highlighted the complexity of the hormonal deregulation.

Surprisingly, 733 olfactory receptor (Olfr) genes were down-regulated in the MetS lung tissue (Supplementary Table 1). Among the top 10 down-regulated genes, 5 of the 10 transcripts

were for Olfrs. These genes can be regulated by the paired box 6 (Pax6) transcription factor or by the glutathione S-transferase fusion protein (Gst) (**Figure 4A-C**). This deregulation may be due to a general inactivation of their transcriptional regulator(s). Alternatively, the deregulation may reflect a change in the number of pulmonary neuroendocrine cells, which are the main Olfr-expressing cells in the lung. Because these cells are potentially responsible for the chemical hypersensitivity feature of several lung diseases, such as COPD, this down-regulation may be related to receptor desensitization or a decrease in the Olfr-expressing cell number in animals with MetS. Further experiments are needed to explore these possibilities.

Ghrelin is another noteworthy molecule that appears among the top upstream regulators (Supplementary Table 2). This peptide influences energy balance and has been detected in the sera of lung cancer patients with cachexia [47]. Similarly, the restablestin-like alpha (Retnla) adipokine is among the top 10 genes and is strongly associated with the inflammatory response and metabolic regulation (Supplementary Table 1). Thus, it is possible to measure Retnla in the serum [48]. Together, Ghrelin and Retnla may comprise one approach for detecting MetS-associated lung damage.

Conclusion

The purpose of our study was to explore the mechanism by which sucrose induces MetS in a rat model and modifies the gene expression and tissue characteristics of the lung. The rat model is characterized by an increase in and the redistribution of retroperitoneal AT, along with biochemical changes in the lipid profile and in leptin and adiponectin levels. These hormonal changes play important roles in establishing a systemic inflammatory response, which can impact the lung's molecular physiology. The lungs exhibit an inflammatory phenotype in animals with MetS. These pathological changes are associated with molecular changes that affect several signaling pathways that are related to melatonin metabolism, olfactory receptors and cytokine production.

Materials and methods

Animals

Control animals (CTL): Twelve healthy male Wistar rats (Rattus norvegicus) (6 months old, 400-500 g) were used. They were fed 50-80 g of a normal rodent diet after weaning (Laboratory Rodent Diet 5001, PMI Nutrition International, Brentwood, MO) for 24 weeks, with water ad libitum; the diet consisted of 28.507% protein, 13.496% fat, and 57.996% carbohydrates HCO (3.7% sucrose, 0.3% fructose, and 0.22% glucose). When they reached a predetermined age, rats were humanely sacrificed by decapitation to obtain the blood and lungs for the experiments. Decapitation was chosen to avoid interference by the anesthetics and to enable exsanguinations. The lungs were excised and washed in cold normal Tyrode's solution (140 mmol/L NaCl, 5 mmol/L KCl, 1 mmol/L $MgCl_2$, 5 mmol/L HEPES, 10 mmol/L glucose, and 1 mmol/L $CaCl_2$, pH 7.4). All solutions were oxygenated with 95% O_2, -5% CO_2 at 160 mmHg pO_2 and 21.3 mmHg pCO_2. Serum was obtained by blood centrifugation. All animals were housed in proper facilities in groups of 6 per cage and maintained at a controlled temperature with an artificial 12:12 hr dark-light cycle.

Animals with metabolic syndrome (MetS)

After weaning at 6 months of age, twelve healthy male Wistar rats were fed the normal rodent diet (Laboratory Rodent Diet 5001, PMI Nutrition International, Brentwood, MO), which consisted of 28.507% protein, 13.496% fat, and 57.996% HCO (3.7% sucrose, 0.3% fructose, and 0.22% glucose); they were also given a 30% sucrose solution as the sole liquid source for 24 weeks. These animals were middle-aged adults by the end of the treatment and were sacrificed as described for the Control group. The lungs were excised and washed in cold normal oxygenated Tyrode's solution. To determine MetS, the body weight, fat tissue weight, blood pressure, triglycerides, total cholesterol, blood glucose, insulin and leptin concentrations were measured as previously described [21].

The MetS group fulfilled the proposed criteria for a definition of MetS for rodents [26].

Of the 25 rats used in this study, 9 (3 for the MetS group, with one technical replicate, and 4 for the control group (CTL), with one technical replicate) were used for the microarray experiment, and 16 (8 in the MetS group and 8 in the CTL group) were used for the histology and validation experiments.

Statement of animal rights and welfare

All procedures were followed in accordance with the ethical standards of the committee for responsible animal experimentation. All animals were lawfully acquired, and the animal procedures in this study was performed in accordance with "The Code of Ethics of the World Medical Association" (Declaration of Helsinki): EC Directive 86/609/EEC for animal experiments [49]. The protocol was reviewed and approved by the Ethics Committee of the National Institute of Cardiology. The experimental studies followed the guidelines of the Norma Oficial Mexicana guide for the use and care of laboratory animals (NOM-062-ZOO-1999) and for the disposal of biological residues (NOM-087-ECOL-1995).

The authors have read the International Association of Veterinary Editors' Consensus Author Guidelines on Animal Ethics and Welfare and declare that all animals in this study were treated according to the aforementioned statement.

Determination of MetS parameters

Blood pressure measurements: Systolic arterial blood pressure measurements were obtained in conscious animals using the tail-cuff method; the cuff was connected to a pneumatic pulse transducer (Narco Bio-Systems Inc., Austin TX) and a programmed electro sphygmomanometer. The recordings were taken from six independent determinations with a Grass polygraph (model 79, Grass Medical Instruments, Quincy, MA).

Determination of morphological variables

Before decapitation, each animal was weighed, and its general health status was assessed. After each animal was sacrificed, the total abdominal adipose tissue was weighed to determine obesity.

Determination of blood variables

After an overnight fast (12 hours), each animal was sacrificed by decapitation, and blood was collected. The serum was separated by centrifugation at 15,000 rpm for 15 min at 4°C and stored at -20°C until further use.

Serum insulin: Serum insulin was determined using a commercial rat-specific radioimmunoassay (RIA) kit (Linco Research, Inc. St. Charles, MO); the sensitivity was 0.1 ng/mL, and the intra- and inter-assay coefficients of variation were 5 and 10%, respectively.

Serum glucose: The glucose concentration was assessed using the commercial DCL-glucose oxidase enzymatic procedure kit (Diagnostic Chemical Limited de México, Mexico).

Serum triglycerides: Triglycerides (TGs) were determined using the commercially available SPINREACT triglycerides-LQ spectrophotometric procedures (Spinreact S. A., Girona, Spain).

Serum cholesterol: Cholesterol was determined using the commercial SPINREACT cholesterol-LQ enzymatic procedure kit (Spinreact S. A. Girona, Spain).

Homeostasis model assessment (HOMA): HOMA was used as an index to measure the degree of insulin resistance and was calculated using the following formula: (insulin (UI/mL)× glucose (mmol/L))/22.5 [50].

Serum leptin: Serum leptin was determined using a specific ELISA (enzyme-linked immunosorbent assay) kit for rat EZRL-83K (Millipore, Co, Billerica, MA); the sensitivity was 0.08 ng/mL. The intra- and inter-coefficients of variation were 2.13 and 2.95%, respectively.

Serum adiponectin: Serum adiponectin was determined using a specific ELISA (enzyme-linked immunosorbent assay) kit for rat EZRADP-62K (Millipore, Co, Billerica, MA); the sensitivity was 0.4 ng/mL. The intra- and inter-coefficients of variation were 1.59 and 6.54%, respectively.

Histological examination of the lung tissue

At the end of the sucrose treatment period, the lungs were fixed in 10% buffered formalin for less than 24 hours and stored in 70% ethanol until paraffin embedding. A portion of each tissue was frozen and protected with Tissue-Tek™, and 4- and 10-μm thick tissue sections were cut from paraffin-embedded blocks and frozen tissue, respectively, for placement onto glass slides. Hematoxylin and eosin (H&E) and Red Oil (RO) staining were performed using standard procedures (INMEGEN, Histology and Confocal Microscopy Laboratory, Mexico).

Total RNA extraction

The RNA isolation from the lung tissues was performed using the Trizol reagent (Invitrogen, Carlsbad, CA, USA) according to the manufacturer's instructions; the RNA from each sample was dissolved in a final volume of 40 μl of RNase-free. Total RNA quantifications and purity assessments were determined with a ND®-1000 spectrophotometer (Technologies, Inc. Wilmington, DE, USA). To determine the total RNA quality, the samples were measured using Agilent's 2100 Bioanalyzer (Agilent Technologies Inc., Santa Clara, CA, USA). An RNA Integrity Number (RIN) ≥6 was used as a quality filter to perform the microarray assays. The samples were stored at -80°C until further processing.

Array experiment

The expression analysis was performed with the GeneChip® Rat 1.0 ST Arrays (Affymetrix, Inc., Santa Clara, CA, USA; http://www.affymetrix.com) using 50 ng of RNA per sample. The target labeling, array hybridization, washing and staining were performed as described in the GeneChip Whole Transcript (WT) Sense Target Labeling manual. The arrays were scanned using the GeneChip Scanner 3000 7G (Affymetrix, Inc., Santa Clara, CA USA).

Data analysis

The raw. CEL files were processed with the Robust Multichip Average (RMA) statistical model for gene expression signals [51]. This algorithm was used for the background correlation, quantile normalization and median polish summarization with the R/Bioconductor software. The comparisons between groups (L_MetS vs. L_C) were performed using R/Limma to obtain the data matrix of the differentially expressed genes that were used for the subsequent analysis [52].

Enrichment analysis

The list of differentially expressed genes was uploaded into the "Ingenuity Pathway Analysis" enrichment tool (IPA, Ingenuity, Inc.; Redwood City, CA, USA). The selection criteria for the analyses included a logarithm of fold change (logFC) ≥1.8 and a $P<0.02$. All data were associated with biological functions and/or diseases, networks, upstream regulators and canonical pathways.

Validation experiments by qRT-PCR

First-strand cDNA synthesis was performed using 2 μg of RNA in a 20-μL total reaction volume using 2.0 μL of 10× RT buffer, 0.8 μL of 25× dNTP mix, 2.0 μL of 10× RT Random Primers, 1.0 μL of MultiScribeTM Reverse Transcriptase, and 4.2 μL of nuclease-free water. The reaction was incubated at 25°C for 5 min, 37°C for 120 min, and 85°C for 5 min, followed by 4°C ∞. The RNA sample was stored in a 10-μL volume (Applied Biosystem, Foster City, CA, USA).

Quantitative Real Time-Polymerase Chain Reaction (qRT-PCR) was used to measure gene expression to validate the microarray technique. TaqMan® probes were used for determining the amplification of the following target genes: Olrf482, Olrf1126, Bcl2l1, Them5 (C2-cd4d), Mrpl41, Pik3c2a, NFKBa and Scl12a2. Hrpt1 was used as the housekeeping gene. The experiments were performed in a 96-well plate from Applied Biosystems ViiA 7 (Carlsbad, CA, USA), and each sample was analyzed in duplicate. The final reactions (10 μl) were set up with 0.5 μl of TaqMan® probes, 5 μl of PCR TaqMan® Universal Master Mix, 2.5 μl of RNase-free water and 2 μl of cDNA (Life Technologies, Carlsbad, CA, USA) according to the manufacturer's protocol. The thermal cycling conditions that were used for all reactions were as follows: Step 1, 50°C for 2 min and 95°C for 2 min; Step 2, 40 cycles of 95°C for 15 sec. The annealing conditions for the sequence-specific oligonucleotide primer were 60°C for 1 min. Gene expression was calculated using the ddCT method that was provided by the Applied Biosystems ViiA 7 software using 10 pooled control rat lungs as a reference sample. Using a method for relative expression, we determined that the fold changes of the analyzed transcripts fell between -1.36 to 4.32; the expression pattern was concordant with the results of the microarray analysis.

Acknowledgements

This work was supported by a PhD scholarship that was received by SMRP from the National Council for Science and Technology (CONACYT #230762, #324898) and by the following financial project: CONACyT, No. project 169652,

"Study of gene expression in the hypothalamus-adipose axis in a rat model with metabolic syndrome", Project manager: Laura del Bosque-Plata, Ph.D. We are thankful for the financial support of the National Institute of Cardiology "Ignacio Chávez" (SSA) for the animal model. We also thank the Histology and Confocal Microscopy Facility and the Gene Expression and Genotyping Facility of the INMEGEN for their support of this investigation.

Disclosure of conflict of interest

None.

Address correspondence to: Laura del Bosque-Plata, Laboratorio de Nutrigenética y Nutrigenómica, Instituto Nacional de Medicina Genómica, Periférico Sur No. 4809, Col. Arenal Tepepan, Tlalpan, C.P. 14610, Ciudad de México, México. Tel: +52(55)53501974; E-mail: ldelbosque@inmegen.gob.mx

References

[1] Alberti KG, Zimmet P and Shaw J. Metabolic syndrome--a new world-wide definition. A consensus atatement from the international diabetes federation. Diabet Med 2006; 23: 469-480.

[2] Ahima RS, Qi Y, Singhal NS, Jackson MB and Scherer PE. Brain adipocytokine action and metabolic regulation. Diabetes 2006; 55 Suppl 2: S145-154.

[3] Ouchi N, Parker JL, Lugus JJ and Walsh K. Adipokines in inflammation and metabolic disease. Nat Rev Immunol 2011; 11: 85-97.

[4] Emanuela F, Grazia M, Marco de R, Maria Paola L, Giorgio F and Marco B. Inflammation as a link between obesity and metabolic syndrome. J Nutr Metab 2012; 2012: 476380.

[5] Tchernof A and Despres JP. Pathophysiology of human visceral obesity: an update. Physiol Rev 2013; 93: 359-404.

[6] Meigs JB, Rutter MK, Sullivan LM, Fox CS, D'Agostino RB Sr and Wilson PW. Impact of insulin resistance on risk of type 2 diabetes and cardiovascular disease in people with metabolic syndrome. Diabetes Care 2007; 30: 1219-1225.

[7] Rask-Madsen C and Kahn CR. Tissue-specific insulin signaling, metabolic syndrome, and cardiovascular disease. Arterioscler Thromb Vasc Biol 2012; 32: 2052-2059.

[8] Adams LA and Lindor KD. Nonalcoholic fatty liver disease. Ann Epidemiol 2007; 17: 863-869.

[9] Luk AO, So WY, Ma RC, Kong AP, Ozaki R, Ng VS, Yu LW, Lau WW, Yang X, Chow FC, Chan JC, Tong PC; Hong Kong Diabetes Registry. Metabolic syndrome predicts new onset of chronic kidney disease in 5,829 patients with type 2 diabetes: a 5-year prospective analysis of the Hong Kong Diabetes Registry. Diabetes Care 2008; 31: 2357-2361.

[10] Esposito K, Chiodini P, Colao A, Lenzi A and Giugliano D. Metabolic syndrome and risk of cancer: a systematic review and meta-analysis. Diabetes Care 2012; 35: 2402-2411.

[11] Bae MS, Han JH, Kim JH, Kim YJ, Lee KJ and Kwon KY. The relationship between metabolic syndrome and pulmonary function. Korean J Fam Med 2012; 33: 70-78.

[12] Naveed B, Weiden MD, Kwon S, Gracely EJ, Comfort AL, Ferrier N, Kasturiarachchi KJ, Cohen HW, Aldrich TK, Rom WN, Kelly K, Prezant DJ and Nolan A. Metabolic syndrome biomarkers predict lung function impairment: a nested case-control study. Am J Respir Crit Care Med 2012; 185: 392-399.

[13] van Huisstede A, Cabezas MC, Birnie E, van de Geijn GJ, Rudolphus A, Mannaerts G, Njo TL, Hiemstra PS and Braunstahl GJ. Systemic inflammation and lung function impairment in morbidly obese subjects with the metabolic syndrome. J Obes 2013; 2013: 131349.

[14] Lee EJ, In KH, Ha ES, Lee KJ, Hur GY, Kang EH, Jung KH, Lee SY, Kim JH, Lee SY, Shin C, Shim JJ, Kang KH and Yoo SH. Asthma-like symptoms are increased in the metabolic syndrome. J Asthma 2009; 46: 339-342.

[15] Adeyeye OO, Ogbera AO, Ogunleye OO, Brodie-Mens AT, Abolarinwa FF, Bamisile RT and Onadeko BO. Understanding asthma and the metabolic syndrome-a Nigerian report. Int Arch Med 2012; 5: 20.

[16] Brumpton BM, Camargo CA Jr, Romundstad PR, Langhammer A, Chen Y and Mai XM. Metabolic syndrome and incidence of asthma in adults: the HUNT study. Eur Respir J 2013; 42: 1495-1502.

[17] Watz H, Waschki B, Kirsten A, Muller KC, Kretschmar G, Meyer T, Holz O and Magnussen H. The metabolic syndrome in patients with chronic bronchitis and COPD: frequency and associated consequences for systemic inflammation and physical inactivity. Chest 2009; 136: 1039-1046.

[18] Akpinar EE, Akpinar S, Ertek S, Sayin E and Gulhan M. Systemic inflammation and metabolic syndrome in stable COPD patients. Tuberk Toraks 2012; 60: 230-237.

[19] Lazovic B, ZS, Mazic S and Đelić M. Prevalence of metabolic syndrome in patients suffered from chronic obstructive pulmonary disease. Journal of Regional Section of Serbian Medical Association in Zajecar 2012; 37: 229-232.

[20] Clini E, Crisafulli E, Radaeli A and Malerba M. COPD and the metabolic syndrome: an intrigu-

ing association. Intern Emerg Med 2013; 8: 283-289.
[21] Castellanos Jankiewicz AK, Rodriguez Peredo SM, Cardoso Saldana G, Diaz Diaz E, Tejero Barrera ME, del Bosque Plata L and Carbo Zabala R. Adipose tissue redistribution caused by an early consumption of a high sucrose diet in a rat model. Nutr Hosp 2015; 31: 2546-2553.
[22] Phillips CM. Nutrigenetics and metabolic disease: current status and implications for personalised nutrition. Nutrients 2013; 5: 32-57.
[23] http://www.fao.org/docrep/w8079e/w8079e0p.htm. F.
[24] Kennedy AJ, Ellacott KL, King VL and Hasty AH. Mouse models of the metabolic syndrome. Dis Model Mech 2010; 3: 156-166.
[25] Fang CS, Wang YC, Zhang TH, Wu J, Wang W, Wang C and Zhang MY. Clinical significance of serum lipids in idiopathic pulmonary alveolar proteinosis. Lipids Health Dis 2012; 11: 12.
[26] Gowdy KM and Fessler MB. Emerging roles for cholesterol and lipoproteins in lung disease. Pulm Pharmacol Ther 2013; 26: 430-437.
[27] van den Borst B, Gosker HR, Koster A, Yu B, Kritchevsky SB, Liu Y, Meibohm B, Rice TB, Shlipak M, Yende S, Harris TB, Schols AM; Health, Aging, and Body Composition (Health ABC) Study. The influence of abdominal visceral fat on inflammatory pathways and mortality risk in obstructive lung disease. Am J Clin Nutr 2012; 96: 516-526.
[28] Lago F, Dieguez C, Gomez-Reino J and Gualillo O. Adipokines as emerging mediators of immune response and inflammation. Nat Clin Pract Rheumatol 2007; 3: 716-724.
[29] Mirrakhimov AE. Chronic obstructive pulmonary disease and glucose metabolism: a bitter sweet symphony. Cardiovasc Diabetol 2012; 11: 132.
[30] Rokni Yazdi H, Lari SM, Attaran D, Ayatollahi H and Mohsenizadeh A. The serum levels of adiponectin and leptin in mustard lung patients. Hum Exp Toxicol 2014; 33: 574-581.
[31] Barnes PJ. The cytokine network in asthma and chronic obstructive pulmonary disease. J Clin Invest 2008; 118: 3546-3556.
[32] Vernooy JH, Ubags ND, Brusselle GG, Tavernier J, Suratt BT, Joos GF, Wouters EF and Bracke KR. Leptin as regulator of pulmonary immune responses: involvement in respiratory diseases. Pulm Pharmacol Ther 2013; 26: 464-472.
[33] Otabe S, Wada N, Hashinaga T, Yuan X, Shimokawa I, Fukutani T, Tanaka K, Ohki T, Kakino S, Kurita Y, Nakayama H, Tajiri Y and Yamada K. Hyperadiponectinemia protects against premature death in metabolic syndrome model mice by inhibiting AKT signaling and chronic inflammation. J Endocrinol 2012; 213: 67-76.
[34] L.A. http://www.lung.org/lung-disease/copd/living-with-copd/nutrition.html?referrer=https://www.google.nl/ Ahwlol-dc.
[35] Forno E, Han YY, Muzumdar RH and Celedon JC. Insulin resistance, metabolic syndrome, and lung function in US adolescents with and without asthma. J Allergy Clin Immunol 2015; 136: 304-311, e308.
[36] Yang Y, Kai G, Pu XD, Qing K, Guo XR and Zhou XY. Expression profile of microRNAs in fetal lung development of Sprague-Dawley rats. Int J Mol Med 2012; 29: 393-402.
[37] Xie Z, Cai L, Li R, Zheng J, Wu H, Yang X, Li H and Wang Z. Down-regulation of miR-489 contributes into NSCLC cell invasion through targeting SUZ12. Tumour Biol 2015; 36: 6497-6505.
[38] Agarwal V, Bell GW, Nam JW and Bartel DP. Predicting effective microRNA target sites in mammalian mRNAs. Elife 2015; 4.
[39] Acuna-Castroviejo D, Carretero M, Doerrier C, Lopez LC, Garcia-Corzo L, Tresguerres JA and Escames G. Melatonin protects lung mitochondria from aging. Age (Dordr) 2012; 34: 681-692.
[40] Galano A, Tan DX and Reiter RJ. Melatonin as a natural ally against oxidative stress: a physicochemical examination. J Pineal Res 2011; 51: 1-16.
[41] Bonnefont-Rousselot D, Collin F, Jore D and Gardes-Albert M. Reaction mechanism of melatonin oxidation by reactive oxygen species in vitro. J Pineal Res 2011; 50: 328-335.
[42] Martins E Jr, Ligeiro de Oliveira AP, Fialho de Araujo AM, Tavares de Lima W, Cipolla-Neto J and Costa Rosa LF. Melatonin modulates allergic lung inflammation. J Pineal Res 2001; 31: 363-369.
[43] De Matos Cavalcante AG, de Bruin PF, de Bruin VM, Nunes DM, Pereira ED, Cavalcante MM and Andrade GM. Melatonin reduces lung oxidative stress in patients with chronic obstructive pulmonary disease: a randomized, double-blind, placebo-controlled study. J Pineal Res 2012; 53: 238-244.
[44] Kim JY, Lee YD, Kim BJ, Kim SP, Kim DH, Jo KJ, Lee SK, Lee KH and Baik HW. Melatonin improves inflammatory cytokine profiles in lung inflammation associated with sleep deprivation. Mol Med Rep 2012; 5: 1281-1284.
[45] Topal T, Oter S, Korkmaz A, Sadir S, Metinyurt G, Korkmazhan ET, Serdar MA, Bilgic H and Reiter RJ. Exogenously administered and endogenously produced melatonin reduce hyperbaric oxygen-induced oxidative stress in rat lung. Life Sci 2004; 75: 461-467.
[46] Maclean MR and Dempsie Y. The serotonin hypothesis of pulmonary hypertension revisited. Adv Exp Med Biol 2010; 661: 309-322.

[47] Shimizu Y, Nagaya N, Isobe T, Imazu M, Okumura H, Hosoda H, Kojima M, Kangawa K and Kohno N. Increased plasma ghrelin level in lung cancer cachexia. Clin Cancer Res 2003; 9: 774-778.
[48] Lee MR, Lim CJ, Lee YH, Park JG, Sonn SK, Lee MN, Jung IH, Jeong SJ, Jeon S, Lee M, Oh KS, Yang Y, Kim JB, Choi HS, Jeong W, Jeong TS, Yoon WK, Kim HC, Choi JH and Oh GT. The adipokine Retnla modulates cholesterol homeostasis in hyperlipidemic mice. Nat Commun 2014; 5: 4410.
[49] http://ec.europa.eu/environment/chemicals/lab_animals/legislation_en.htm Lotpoaufsp.
[50] Matthews DR, Hosker JP, Rudenski AS, Naylor BA, Treacher DF and Turner RC. Homeostasis model assessment: insulin resistance and beta-cell function from fasting plasma glucose and insulin concentrations in man. Diabetologia 1985; 28: 412-419.
[51] Bolstad BM, Irizarry RA, Astrand M and Speed TP. A comparison of normalization methods for high density oligonucleotide array data based on variance and bias. Bioinformatics 2003; 19: 185-193.
[52] Wettenhall JM and Smyth GK. limmaGUI: a graphical user interface for linear modeling of microarray data. Bioinformatics 2004; 20: 3705-3706.

Supplementary Table 1. Top 10 molecules. Log ratio up-regulated and Log ratio down regulated

Molecules	Exp. Value	Molecules	Exp. Value
Them5	1.3	Loc685792	-2.977
H2-t22	0.982	Sult1c2	-2.707
Retnla	0.960	Sult2a	-2.369
Rpl12	0.940	Olfr1306/Olfr1307	-2.358
Trim16	0.769	Amy2b	-2.330
Zbtb16	0.735	Olfr1245	-2.185
Nrn1	0.654	Olfr484	-2.151
Sbsn	0.618	Olfr910/Olfr912	-2.122
Scd	0.612	Olfr823/Olfr824	-2.111
Pfkfb1	0.611	Tceb1	-2.048

Supplementary Table 2. Top upstream regulators

Upstream Regulator	*p*-value of overlap
Ghrelin	6.03E-03
PXR ligand-PXR-retinoic acid-RXR	1.94E-02
Bcl11b	2.45E-02
5-4-N-methyl-N2-pyridylamino ethoxybenzyl thiazolidine-2,4-dione	2.50E-02
Slc34a3	2.52E-02